

Comparative Distortion Analysis of Welded T-Joint between 2D-Shell and 3D-Solid Element using FEA with Experimental Verification

*Keval. P Prajadhiana**, *Yupiter HP Manurung*, *Muhammad Zohdi bin Zainir*, *Omar Yahya*, *Juri Saedon*, *Mohd Shahrman*, *Abdul Rahman Omar*
and *Wahyu Kuntjoro*

Faculty of Mechanical Engineering, UiTM Shah Alam

Khairulnizam bin Kasim

Politeknik Sultan Salahuddin Abdud Aziz Shah, Shah Alam

Dendi P. Ishak

Department of Industrial Engineering, University of Indonesia, Depok, Indonesia

Alexander Bauer and Marcel Graf

Professorship of Virtual Production Engineering, Chemnitz University of Technology, Germany

**Keval.priapatama@gmail.com*

ABSTRACT

In this paper, three different finite element simulations of welded T-Joint are to be computed using 2D-shell and 3D-solid element types. The assigned element types are built and modelled on T-joint plate with thickness of 4 mm. The thermo-mechanical FEM simulation using MSC Marc/Mentat is implemented throughout the analysis. The angular distortion induced by welding process on the web is to be analysed under similar heat input and clamping condition on the stiffener. The selected heat source model is Goldak's double ellipsoid which is normally used for arc welding processes. In order to verify the simulation process, selected one-pass and double-sided GMAW process with fully automated experimental procedure was conducted using the exactly similar parameters assigned in FEM simulation. A measurement point analysis is further carried out to assess the displacement value of the actual T-Joint welding process by using

Coordinate Measuring Machine (CMM) and to compare with the result of FEM simulation. It is found out that, for this kind of joint design and geometry, conducted FEM procedure shows good agreement on distortion tendency of the web within the range of percentage error up to 20%. However, the element types shell and solid without table do not indicate significant difference in simulation result compared to solid element with table.

Keywords: *Finite Element Method; Welding Simulation, Distortion, T-Joint*

Introduction

The basic principle of fusion welding process is that two or more materials with similar or dissimilar composition heated until their melting point then connected among each other after the cooling phase commenced. One of the sculptural fusion welding processes is GMAW used commonly due to its flexibility and high range of productivity in engineering field with an extensive range of plate thickness [1-3]. Presence of distortion in the weldments affects the dimensional accuracy causing misalignment of structural parts, which leads to poor joint fit-up and decreases aesthetic value. Even though welding process has been used frequently in manufacturing environment, the distortion that occurs could lead to the imperfect final product design that would increase the production cost in overall, especially on maintenance cost [4]. Distortion in the welding process resulted from the unbalanced thermally induced stress that exists in non-restrained weld joints. The three major distortion forms that usually found in welding processes are: (1) longitudinal shrinkage that takes place in a direction parallel to the weld line, (2) transverse shrinkage that develops in a direction perpendicular to the weld line and (3) angular change due to rotation around the weld line. Configuration of weld joint, heat input during transfers and welding sequences are factors that could affect the extend of distortions [5].

Finite Element Methods (FEM) is a numerical approach analysis of a model component. In welding simulation, the principle of Finite Element Analysis consists of two parts, which are thermal and mechanical analysis [6]. The temperature calculation is determined as the variable for each melting and cooling points in thermal analysis [7]. Since its introduction, the numerical simulations have become a mandatory equipment on predicting the outcome of the real experiment prior to field action. The 3D model usage becomes a necessity for the high-accuracy prediction of post-weld deformation and stress distribution on the joint.

However, the limitation of computational ability is a minor constraint on predicting the outcome that 100% accurate compared to real model. The numerical simulations that specified for reducing the

computational time and complexity of transient linear-problem has been an interest for researcher in FEM area for years [8]. Mato and Zdenko [9] had performed an analysis based on T-joint weld aiming to analyse residual stresses and distortions induced by T-joint weld and found that the numerical model of 3D-solid and 2D-shell had no significant influence towards the temperature distribution field.

Therefore, welding distortion is supposed to be estimated, particularly prior to the initiation of real welding process in order to reduce or avoid the setback, minimize the negative effects, enhance the quality of welded structures, and, more importantly, reduce the outlay on capital expenditure [10]. This research will deal with three double-sided T-joint distortion analysis between 2D-Shell, 3D-Solid element types with and without welding table, which will be later compared with experimental investigation by using fully automated equipment and procedure.

Simulation Procedure using Nonlinear FEM

Weld Modelling and Simulation using MSC Marc/Mentat

The most modern simulation technique of the actual manufacturing process is considered as an advanced phase of modern engineering since it combines all the aspects of thermal, mechanical and metallurgical phenomena in one numerical model. Numerous researchers [11-12] has applied FEM on analysing the distortions of the weldment in thermoelastic-plastic behaviour in order to deal with such a complex simulation in an efficient manner. The general flowchart of simulation process using MSC/Marc is exhibited in Figure 1.

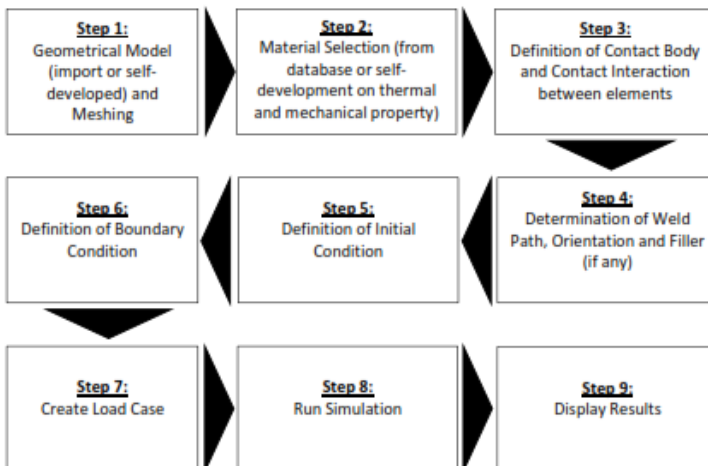


Figure 1 : General Flowchart of Simulation Procedure using

MSC Marc/Mentat

Geometrical and Material Description

Figure 2 shows the schematic illustration of the geometrical model, which have the dimension of 100x150mm as web and 50x150mm as stiffener plate. The thickness of plates is 4mm, which was assigned to produce double-sided weld. In this simulation, the geometry is meshed using single-passed welding bead.

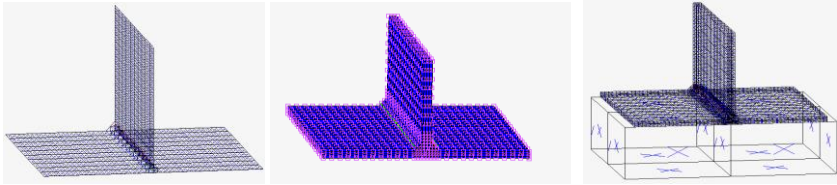
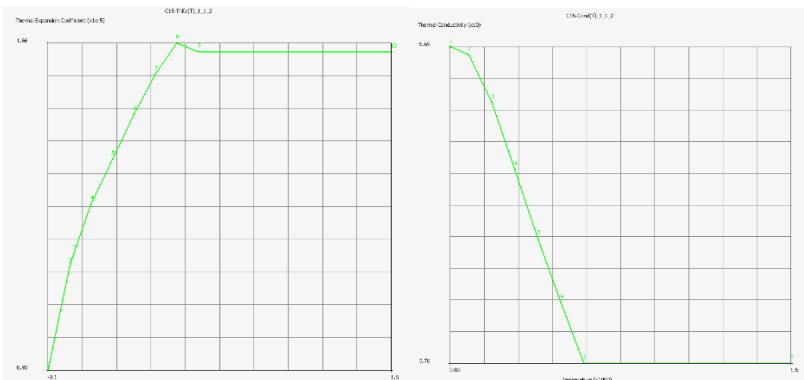


Figure 2 : Finite element models of 2D-Shell (left), 3D-Solid T-joint without table (middle) and 3D-Solid T-joint with table (right)

MSC Marc/Mentat has a capability to act independent from the 3rd party CAD based software since geometry can be modelled using own platform. By looking at this simplified feature, the drawing phase could be done faster using MSC Marc/Mentat, although it also provide the import option from 3rd party CAD software.

In this simulation, the C15 steel is selected as material for the T-joint plates and filler material. The physical properties of the material are shown in Figure 3. This figure shows that the material assigned for the FEM simulation has temperature-dependent variables.



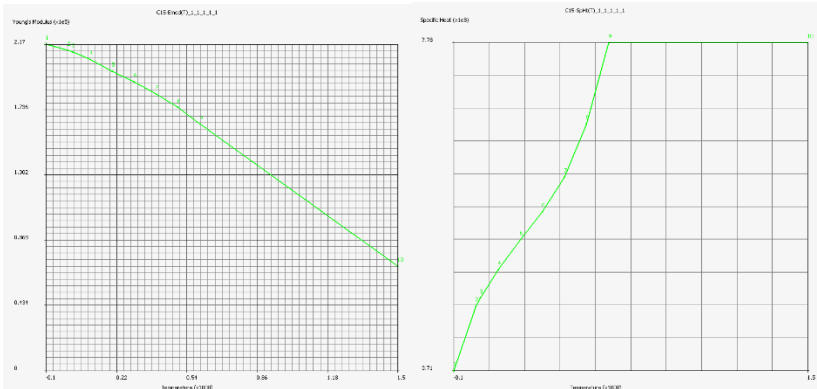


Figure 3 : Temperature-dependant thermo-physical properties of C15 (clockwise direction: Thermal Expansion Coefficient, Thermal Conductivity, Young’s Modulus and Specific Heat)

Assigning Contact Body and Interaction

Contact Bodies are set prior determining the contact interaction of all the elements that found in this FEM Simulation. Four sections of elements appears in this simulation are Plates, Weld Filler and Table. Deformable type of contact is assigned to both weldment and filler while rigid type of contact to table. This applies for both Shell and Solid model. In this FEM simulation, the deformable contact type influenced by the result of the simulation after the job has been set, the alteration could be seen implicitly during thermomechanical analysis where the surface transformation occurs while running the results. While rigid contact tends to have more static surface during the execution because rigid body mode is defined as the free translation or rotation of a body without undergoing any significant internal deformation [13].

There are two types of contact interaction namely “Touching/T” and “Glued/G”. These two contacts are available in MSC Marc/Mentat located on contact bodies section. In a structural analysis, a touching condition triggers the local application of a non-penetration constraint still allowing relative sliding of the bodies in the contact interface. While a glued condition suppresses all relative motions between bodies through boundary conditions applying them to all displacement degrees of freedom of the nodes in contact. For elements with nodes that also have rotational degrees of freedom, the rotations may be additionally constrained to provide a moment carrying glue capability [14].

Table 1 : Contact interactions of elements (G: Glued, T:Touching)

Nr.	Component Name	1	2	3	4	5
1	Plate 1		T	G	G	T
2	Plate 2	T		G	G	T
3	Weld Filler 1	G	G			
4	Weld Filler 2	G	G			
5	Table	T	T			

Initial and Boundary Conditions

The initial and boundary conditions of a finite element model includes thermal and mechanical boundary conditions, in which the main consideration of the thermal boundary conditions is heat radiation, heat conduction and convection thermal cooling [15]. In this simulation, the analysis of boundaries are divided into Thermal and Structural analysis. The thermomechanical parameters are defined in each sections of boundary condition on both shell and solid model.

The structural analysis for this boundary consists of fixed displacement and structural point load. Both are the features of structural analysis provided by MSC Marc/Mentat. The main consideration of the mechanical boundary conditions is to simulate the constraints of the fixtures on the workpiece during the welding process and the constraints of removing the fixture after cooling to room temperature [16]. In structural fixed displacement, there are two things that need to be done which are fixed the table so that there is no movement allowed, but for the base metal, the Y-axis is allowed to move. This boundary condition is assigned in order to compliment the rigid contact applied on the Table element which makes the table is not allowed to move during the execution of welding process.

The point load available in FEM analysis of MSC Marc/ Mentat acts as the point of which the clamping is located. As for the clamping condition, Figure 4 demonstrates the clamping placement as well as the boundary condition that is assigned within the clamping. Clamping force is applied with the direction points to negative Y direction applied for both point load clamping. The placement for both clamps are in similar locations with the experimental welding.

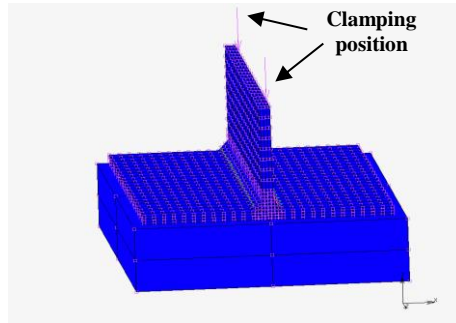


Figure 4 : Clamping position of structural boundary condition

The thermal boundary condition in this simulations are Thermal Face Film and Thermal Volume Weld Flux. The Thermal Face Film is implemented in the same procedure for both Shell and Solid model of T Joint while Thermal Volume Flux has one of the two models differs from each other. This face film need as boundary condition in welding process because of the calculation for heat transfer from nodes to other nodes is needed whether in deformable to rigid body or deformable to deformable body. In addition to this, film coefficient and the value for ambient temperature need to set in the simulation so that there is heat transfer between the surrounding environment and surface. The value of ambient temperature is 20°C and the values of the film coefficient and contact heat transfer coefficient are 25 W/m²K and 1000 W/m²K respectively.

In shell geometry, two weld fluxes are mandatory to be added (face weld flux and vicinity face weld flux) that need to apply which were for the weld filler and vicinity area of the weld filler. In this case, the heat to the surrounding of weld filler (vicinity face weld flux) was assumed as nothing. The amount of heat input that being used was 2.7×10^6 N*mm/s and the amount of efficiency being used is 80%. The velocity of weld speed matches with the experimental parameter which is 5 mm/s which would be later accompanied by weld path and filler assignation.

Table 2 displays the parameters that are implemented on the simulation process that would be later used on the experimental verification. The Current (I) and the Voltage (V) are considered under the equation of power. The assigned travel speed (v) was based on the ideal welding speed for this material using one-pass T-joint.

Table 2 : Welding parameters used in Simulation

Welding Parameter	Value
Current, I (A)	150
Voltage, V (V)	18
Travel Speed, v (mm/s)	5

Heat source generation in MSC Marc/Mentat is set while assigning the Volume Weld Flux boundary condition in thermal analysis. The Goldak's Double Ellipsoid Model is chosen as the heat source model for this simulation. The Double Ellipsoid Model that mostly used to represent the heat which is made by the torch in GMAW welding. Double Ellipsoid means that the heat source is consisted of two elliptic regions, one in front of the arc and one is in the centre. $Z > 0$ and the other behind the arc centre is $Z < 0$ [17]. The Figure 5 illustrates the Goldak's Double Ellipsoid model.

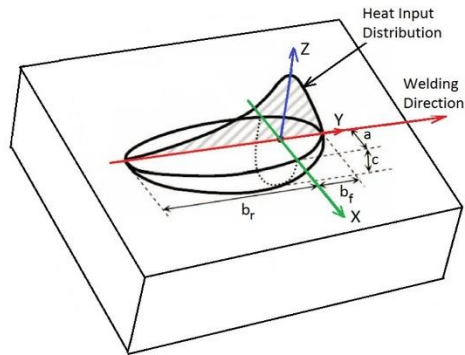


Figure 5 : Illustration of Goldak's Double Ellipsoid Heat Source Model

Pavalec in late 1960s recommended a heat source model of circular disc with Gaussian distribution on the surface of the workpiece. Then, Goldak double ellipsoidal heat source was developed for the use of FE in welding simulation process. This model incorporated the heat below the welding arc resulting an accurate welding simulation for deep and shallow penetration. The Goldak double ellipsoidal model is a widely used heat source model for GMAW welding process in manufacturing environment nowadays [18].

The power density of the heat flux in front section (Q_{vf}) of heat source can be determined by following formula (Eq 1):

$$q_{vf}(x, y, z) = \frac{6\sqrt{3}f_f Q}{abc_f \pi \sqrt{\pi}} e^{-3\frac{x^2}{a^2}} \cdot e^{-3\frac{y^2}{b^2}} \cdot e^{-3\frac{z^2}{c_f^2}} \quad (1)$$

And the power density of the heat flux in rear section (q_{vr}) can be determined by (Eq 2):

$$q_{vr}(x, y, z) = \frac{6\sqrt{3}f_r Q}{abc_r \pi \sqrt{\pi}} e^{-3\frac{x^2}{a^2}} \cdot e^{-3\frac{y^2}{b^2}} \cdot e^{-3\frac{z^2}{c_r^2}} \quad (2)$$

Where f_f and f_r are the heat deposited fractional factors in the front and rear quadrant respectively and its sum is equal to 2. The distribution of fluxes in the double ellipsoid model is determined by 4 directions: Width (b), Depth (d), Rear Length (ar) and Front Length (af). The values for each directions are shown in Table 3.

Table 3 : Heat Source Dimension in FEM Simulation

Heat Source Direction	Value
Width (mm)	3
Depth (mm)	1
Rear Length (mm)	2.5
Front Length (mm)	1.5

Figure 6 demonstrates the calibration of heat source model implemented in FEM simulation.

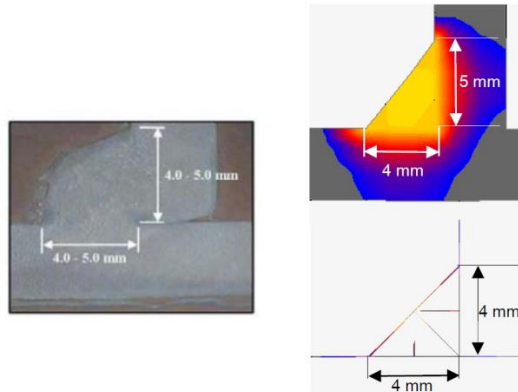


Figure 6 : Heat Source Model calibration from experiment (left), solid model (right, upper) and shell model(right, below)

Experimental Set Up and Procedures

A series of comprehensive experimental welding processes were conducted in order to verify the simulation FEM result using T joint weldment. Robotic Welding machine used for this experiment is ABB IRB 2400/16, with the GMAW power source KEMMPI Pro Evolution ProMIG 540MXE. The demonstration of robotic welding equipment can be seen in figure 7. Robotic welding is recognized these days as a mature production method which has a flexible movement pattern using certain axes.



Figure 7 : Robotic welding apparatus: ABB IRB 2400/16, KEMMPI ProMIG 540 MXE and shielding gas (80 % Ar and 20 % CO₂)

The low carbon steel material is selected in the experimental process. This type of material has been used in many real-life manufacturing process especially in welding sector due to the flexibility of the structure with the guaranteed strength and quality. Table 4 shows the chemical composition

based on material data sheet and the experimental results obtained using an Arc Spark Emission Spectrometer.

Table 4 : Chemical Composition of Material

Elements	C15 (Material Data Sheet)	Low Carbon Steel (Arc Spark Spectrometer)
C	0.12 – 0.18	0.186
Mn	0.3 – 0.6	0.146
Si	< 0.4	0.011
S	< 0.045	0.0011
P	< 0.045	0.001

Robotic welding system has an advantage as a single point remote robot control unit which can be applied to perform any kind of possible welding parameter and automated robot programming [19]. The dimension of T-joint is similar to welding simulation. Parameters being set for this validation is applied according to the parameters that were assigned in the FEM simulation, which can be seen in Table5 below.

Table 5 : Welding parameters used in experiment

Welding Parameter	Value
Current, I (A)	140 - 160
Voltage, V (V)	17-20
Travel Speed, v (mm/s)	5
Shielding gases (Ar/CO ₂)	80%, 20%

A precision Coordinate Measuring Machine (CMM) from Mitutoyo model Beyond 70 with probe system model Renishaw PH9 is used as measurement for distortions of each point on the weldment surfaces. After the welding process, the specimens were quantified using the same CMM to obtain the final readings of the points identical to those that have been measured before. Two measuring points of the joint were established in order

to have the CMM machine detect the distortion on certain point that are going to be analysed.

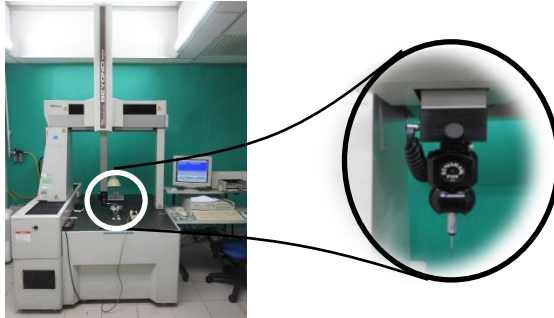


Figure 8 : Coordinate Measuring Machine (CMM) Mitutoyo Beyond 707

Result and Discussions

Figure 9 and 10 demonstrate the angular distortion results towards the displacements of both shell and solid model of FEM simulation. The visualization set in MSC Marc/Mentat is Countour Band setting view and its applied for both shell and solid model. By looking at these pictures, the distribution of stress on the weldment surface can be examined through the deformed shape and colours in a weld specimen.

Figure 10 displays the experimental result of distortion of the T joint. The solid model has two different models to be tested which are with table and without table model. The table acts as the fixed displacement on both x and z axis under the plate which determines the bearing condition of the weldment, while the one without table has the fixed displacement placed entirely on the bottom of the plate which act as the bearing for the weldment.

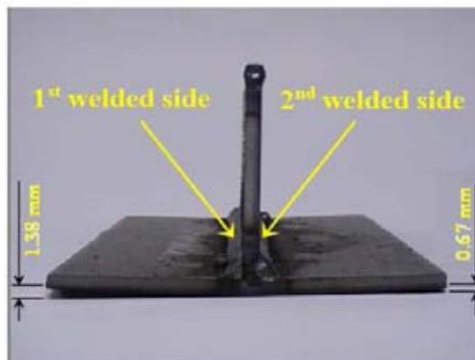


Figure 9 : Distortions result in T-join experiment

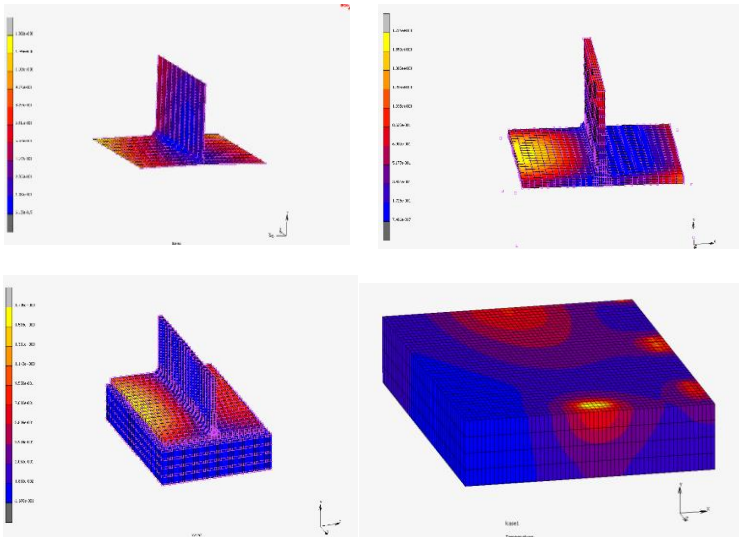


Figure 10 : Distortion results for 2D-Shell (upper left) and 3D-Solid without table (upper right), 3D-Solid with table (bottom left) and temperature reaction within table (bottom right)

From the graph above it can be shown there is a shape difference between both shell and solid model and also solid table which has table on it, these different conditions would affect the value of distortion which lead to a conclusion that difference in geometric model could differs the final FEM simulation results. The image bottom right image shows the temperature reaction within the table of FEM simulation, means that there is reaction and change in the structure of FEM based table. Table 6 exhibits the comparison details of real life experiment model that will be compared against FEM simulation. The number that were gathered for the experiment result are from the measurement machine (CMM). By utilizing CMM, the percentage of distortion in a certain nodes were calculated, the same nodes also pointed in the FEM simulation. Table 7 displays the needed CPU-Time to execute the simulation of three model types.

Table 6: Simulation and experiment result comparison

Joint Sequence	Average Distortion [mm]				Relative Percentage error [%]		
	Experiment	2D-Shell	3D-Solid without Table	3D-Solid with Table	2D-Shell	3D-Solid without Table	3D-Solid with Table
1 st side	1.38	1.14	1.18	1.20	17.3	14.4	13.7
2 nd side	0.67	0.74	0.79	0.61	19.4	18.4	9

Table 7 : CPU-Time needed for simulation

Model Type	CPU-Time (s)	Relative Percentage Difference [%]
2D-Shell	72	1
3D-Solid without Table	109	51,3
3D-Solid with Table	414	475

By looking on the weld deformation formed by numerical analysis, it can be seen that the precision mostly appears on the geometry near the weld bead. A really careful approach need to be done while determining the weld bead size for a better final result. Based on this FEM simulation, it can be concluded that variation in physical properties, thickness, chemical composition and the specimen of material could lead to the result's deviation when it compared with the experimental result.

Conclusion

Through the Finite Element Method, a study of distortions of T Joint weld using Gas Metal Arc Welding (GMAW) had been executed. The research covers both numerical and experimental analysis which was compared as final output of this research. The software MSC Marc/Mentat is used for all numerical analysis of both shell and solid element types. To conclude this research, there are some crucial points that will be explained by following statements:

1. The FEM analysis of T-joint model were executed successfully and the simulation procedure is clear as well as structured,
2. For this joint type, the simulation results show insignificant dependency on selection of element type.
3. Simulation using MSC Marc/Mentat shows good agreement on distortion tendency compared to the results of experiment with relative percentage error up to only 20%.
4. The best simulation result (error of 9-13.7%) is the model with table under consideration of heat transfer to the environment and to the contacted table.
5. The fastest CPU-time is however the shell model with 72 seconds. T-joint without and with table had percentage difference of 51% and 475% respectively relative to shell model. The T Joint with table has the longest CPU time due to more elements needed to be calculated on the table and contact heat transferred from the weldment to the table.
6. The non-homogenous material, geometry, pre-condition of welding process and the fluctuating parameters during experimental analysis, might cause the difference between simulation and experiment results.

From the knowledge point of view, important information through simulation could be obtained which can be used as a planning tool within the design phase or prior to actual welding process. This investigation could bring a contribution towards the further development of research in Virtual Manufacturing area such as by considering the material behaviour and modelling.

Acknowledgement

The authors would like to express their gratitude to staff member of Welding Laboratory, Advanced Manufacturing Laboratory and Advanced Manufacturing Technology Excellence Centre at Faculty of Mechanical Engineering, Universiti Teknologi MARA (UiTM) for encouraging this research. The simulation was carried out at our partner university Chemnitz University of Technology in Germany under international research grant of DAAD (Ref. Nr.: 57347629). This research is also financially supported by Geran Inisiatif Penyeliaan (GIP) from Phase 1/2016 with Project Code: 600-IRMI/GIP 5/3 (0019/2016).

References

- [1] Tso-Liang Teng, Chin-Ping Fung, Peng-Hsiang Chang, and Wei-Chun Yang, Analysis of residual stresses and distortions in T-joint fillet welds, Chong Qing University (2014)
- [2] Long H, Gery D, Carlier A, Maropoulos PG .prediction of welding distortion in butt joint of thin plates. *Mates* (2012) 30:4126
- [3] Lu Y, Wu P, Zeng J, Wu X, Numerical simulation of welding distortion using shrinkage force approach and application. *AdvMate*, (2011).
- [4] Tapas B, H Chaledurai, Zahid A. Experimental investigation and numerical analyses of residual stresses and distortions in GMA welding of thin dissimilar AA5052-AA6061 plates. *Journal of Manufacturing Processes* (2017) :25-340–350.
- [5] Messler Jr RW. Principles of Welding. New York: John Wiley & Sons Inc; (1999). p. 181–97.
- [6] Deng D, Liang W, Murakawa H. Determination of welding deformation in fillet welded Joint by means of numerical Simulation and Comparison with Experimental Measurements. *J Mater Process Technol* (2012);183:219–25.
- [7] Barsoum Z, Lundback A. Simplified FE welding simulation of fillet welds – 3D effects on Formation Residual Stresses. (2011);16:2281–9.
- [8] Welding consumables – wire electrodes and weld deposits for gas shielded metal arc welding of non-alloy and fine grain steels – classification. EN ISO14341; (2011).
- [9] Mato P, Zdenko T, et al. Numerical analysis and experimental investigation of welding residual stresses and distortions in a T-joint fillet. *Materials and Design Journal* 53, 1052-1063, (2014).
- [10] Yupiter HPM, Shahar M, et al. Investigation on welding distortion of combined butt and T-joints with 9-mm thickness using FEM and experiment. *International Journal Advanced Manufacturing Technology* 77:775–782, (2014).
- [11] Bradac Josef. Numerical analysis using in production of welded parts. *Acta Technica Corviniensis Buletin of Engineering* (2010) :89e93.
- [12] Lidam Robert Ngendang, et al. Simulation study on multi-pass welding distortion of combined joint types using thermo-elastic-

- plastic FEM. The Journal of Engineering Research June (2012)
;9(2):1e16.
- [13] Batchu, Surya. Usage of The Rigid Body Model in Finite Element Analysis. Stress E Book LLC. (2015).
- [14] MSC Team . Marc Mentat 2015 User Guide Documentation Vol A. MSC Software (2015).
- [15] G Mi, C Li , et al. Finite Element Analysis of Welding Residual Stress of Alumunium Plates Under Different Butt Joint Parameters. Engineering Review, Vol. 34 Issue 3 (2014).
- [16] Goldak, J., Bibby, M., Downey, D., Gu, M., Heat and fluid flow in welds, International Institute of Welding Congress on Joining Research, Advanced Joining Technologies, Chapman and Hall, (2000).
- [17] J. Bradac, “Calibration of Heat Source Model in Numerical Simulation of Fusion Welding”, *Machines, Tehnologies, Materials*, Issue 11, ISSN 1313-0226 ,(2013).
- [18] P. S. Minh, T. V. Phu, “Study on the Structure Deformation in the Process of Gas Metal Arc Welding (GMAW)”, *American Journal of Mechanical Engineering*, (2014), Vol. 2, No. 4, 120-124.
- [19] Weman K, Lindén G. MIG welding guide. Woodhead Publishing Limited, Cambridge (2006).